Organic & Biomolecular Chemistry

Accepted Manuscript

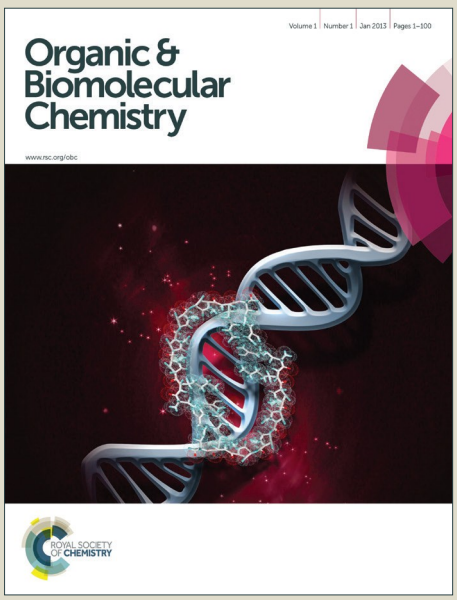

ROYAL SOCIETY OF CHEMISTRY

www.rsc.org/obc

Journal Name

ARTICLE

Cyanine Fluorophore for Cellular Protection Against ROS in Stimulated Macrophages and Two-Photon ROS Detection

Received 00th January 20xx,
Accepted 00th January 20xx

DOI: 10.1039/x0xx00000x

www.rsc.org/

M. S. Chan,[a, †] D. Xu,[b, †] L. Guo,[b] D. Y. Tam,[a] L. S. Liu,[a] M. S. Wong*[b] and P. K. Lo*[a]

We report the first example of a novel two-photon active, biocompatible, and macrophage cell-membrane permeable carbazole-based cyanine fluorophore for detection of three biologically important ROS namely, $^{\cdot}OH$, O_2^- and OCl^- in solution. This versatile probe shows cellular protection not only in stimulated macrophages from phorbol-12-myristate-13-acetate-induced morphological change but also lipopolysaccharide-induced cytotoxicity by quenching with the O_2^- and OCl^- production, respectively. Such protection could be visualized by a distinct change in fluorescence intensity of the probe.

Introduction

Oxidative stress is typically an imbalance between the production of reactive oxygen species (ROS) and antioxidant defences. Excessive production of ROS easily oxidizes protein, induces DNA damage, impairs mitochondria functions, and influences cell division, resulting in serious cellular injury.[1] Thus, ROS are non-trivial molecules in terms of regulating a wide range of physiological functions including immune response[2] and cell signaling.[3] They also play a pivotal role as causative agents in the pathophysiology of a large variety of human diseases, including cancers,[4] cardiovascular diseases,[5] neurodegenerative disorders[6] and ischemia-reperfusion (IR) injury in surgery.[7] Scientists have made use of organic nitrone spin traps to react with reactive free radicals to form a spin adduct with longer half-live for, monitoring ROS concentrations, elucidating their biological roles and underlying molecular mechanism by electron paramagnetic resonance (EPR) measurements.[8-9] However, diamagnetic ROS including H_2O_2, and hypochlorite anion are not applicable.[10] In addition, no direct and obvious signal is obtained for monitoring of ROS and reflecting of cellular protection effects. One simple way to overcome this hurdle is to develop a novel ROS sensor which reacts with potent ROS completely and furnishes a change of its fluorescence intensity for direct detecting and imaging of ROS. Subsequently the change in fluorescence intensity of ROS sensor should reflect a direct indication of cellular protection in terms of preventing accumulation of toxic oxidation products and cytotoxicity in mammalian cells. Regarding biological applications, utilizing two photon (TP) fluorescence microscopic technique would allow deeper tissue penetration (>500 μm), eliminate tissue autofluorescence and self-absorption, and reduce photobleaching and photodamage[11-12] which are particularly important for prolong biological studies, and thus has become an indispensable imaging tool, especially for medical diagnostics.[13] Among various reported TP fluorescence probes,[14-18] there is no report published on the use of two-photon fluorescent probes to detect and deactivate ROS for cellular protection of endogenous stimuli-induced macrophage. In addition, development of useful TP fluorescent ROS sensor or scavengers with good solubility in aqueous media without aggregation and low cytotoxicity for biological applications in living systems still remains a great challenge.

To meet such demands, we report herein the design, synthesis and photophysical evaluation of a novel carbazole-based cyanine, namely SPC as a simple and highly specific fluorescent probe for detecting $^{\cdot}OH$, O_2^- and OCl^- under ambient conditions, concomitant with a strong decrease in fluorescence. More importantly, the probe is cell membrane permeable to macrophages, pH stable and non-cytotoxic. Its applicability for one-photon and two-photon imaging of OCl^- and O_2^- in stimulated macrophages has been demonstrated. More importantly, SPC exhibits a protection capability to prevent the phorbol-12-myristate-13-acetate (PMA)-induced morphological changes of RAW264.7 cells as a function of time as well as to block the lipopolysaccharide (LPS)-induced cytotoxicity of RAW264.7 cells in a dose-dependent manner. Although cyanine fluorophores have been widely investigated for various fluorescent probes, no report has been made on ROS quenching, imaging and cellular protection yet.

[a] Department of Biology and Chemistry, City University of Hong Kong, Tat Chee Avenue, Kowloon Tong, Hong Kong SAR, China. E-mail:peggylo@cityu.edu.hk; Tel:+852 34427840
[b] Department of Chemistry and Institute of Molecular Functional Materials, Hong Kong Baptist University, Kowloon Tong, Hong Kong SAR, China. E-mail:mswong@hbu.edu.hk; Tel: +852 34117069
† These authors contributed equally to this work.

Electronic Supplementary Information (ESI) available: Results of physical measurements for SPC, synthetic details, and ^1H NMR and ^{13}C NMR and HRMS spectra. See DOI: 10.1039/x0xx00000x

Results and Discussion

Synthesis and characterizations of carbazole-based cyanine, SPC

Synthesis of SPC, adopting the previously published protocols [19-21] is outlined in Scheme S1. All of the intermediates and SPC were fully characterized using ^{1}H NMR, ^{13}C NMR and HRMS (Figs. S1–3). The data obtained are in good agreement with the proposed structures (Fig. 1). SPC is highly soluble in common organic solvents and in phosphate buffer (Table S1 and Figs. S4-5). The absorption maximum is observed at 423 nm and 431 nm in phosphate buffer and in DMSO, respectively. Upon excitation at the absorption maximum, SPC exhibits relatively strong fluorescence at 563 nm in DMSO but very weak and red-shifted emission (~ 575 nm) in phosphate buffer due to the more stabilized charge transfer excited state. More importantly, SPC exhibits a strong two-photon excited absorption with a band peaked at 810 nm, analogous to that of SPM (δ_2 = 430 GM at 850 nm in PB)[19] (Fig. S6). Moreover, this probe was found to be stable in aqueous media at a wide range of pH spanning from pH 4 to pH 10 in which the fluorescence intensity was stable over a period of 24 h in ambient conditions (Fig. S7). This property is particularly beneficial to the application as a biological fluorescence probe under physiological conditions.

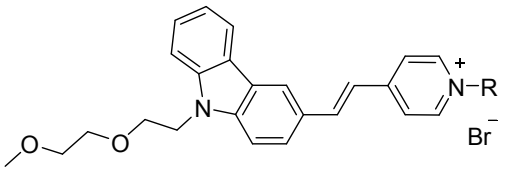

SPM: R = CH_3
SPC: R = CH_2COOH

Fig. 1 Chemical structures of SPC and SPM.

Reactivity and selectivity of SPC toward reactive oxygen species (ROS)

To evaluate the reactivity and selectivity of SPC toward ROS, we investigated fluorescent response upon addition of various ROS including H_2O_2, $^{1}O_2$, OCl^-, O_2^-, $^{\cdot}OH$, $ONOO^-$, NO_2^-, NO_3^-, TBHP, and cysteine (thiol species) as well as metal ions including Ca^{2+}, Na^+, K^+, Ba^{2+}, Fe^{3+}, Fe^{2+} and Cu^{2+}. These selected metal ions are biologically relevant species which play vital roles in regulating and maintaining proper cellular environment such as redox environment in mitochondria for cell activities and functions including a controlled enzyme-catalyzed reaction. The reaction was conducted at ambient temperature and the fluorescence intensity was monitored over time. As shown in Fig. 2A, the fluorescence change indicated that SPC probe selectively reacted with $^{\cdot}OH$, O_2^-, and OCl^- over a period of 24 h. The rest of the tested ROS shows very little quenching effect on SPC. To further investigate the chemical kinetics, several reaction time points were examined. As shown in Fig. 2B, the fluorescence of SPC was completely quenched by $^{\cdot}OH$, O_2^-, and OCl^- after 3 min, 3 h and 24 h, respectively under the experimental conditions. Nevertheless, the reaction kinetic in the cellular conditions are much faster, it is highly feasible to use the SPC probe to monitor these ROS at a real-time scale. Fig. 2C shows the fluorescence emission spectra taken from SPC as a function of O_2^- concentration. As expected, the fluorescence intensity of the probe decreased progressively with an increase of the O_2^- concentration. Moreover, when reacted with fixed amount of O_2^- (8 mM), the absorption and emission maximum intensity of SPC probe decreased as a function of time, accompanied with distinguishable colour change from yellow to very pale orange after 3 h (Figs. S8 and 2D, blue dots). Nevertheless, it is not feasible to determine its reactivity/selectivity toward $^{\cdot}OH$, O_2^-, and OCl^- by means of competition study as the preparations of the three ROS are not compatible. To get an insight into the chemical role of SPC in the reaction with O_2^-, the spectroscopic techniques including ^{1}H NMR, HRMS and UV-Vis were used to probe the reaction. The reaction was performed with 10 mM SPC and 40 mM O_2^- in D_2O. The proton resonance of the double bond of SPC in the ^{1}H NMR spectrum disappeared after 3 h of reaction, indicating that the double bond in the probe was cleaved by O_2^-, forming a diagnostic marker product, hydroxyl-SPC which shows a base peak at m/z 449.2098 corresponding to $[M]^+$ in the HRMS measurement. (Figs. S9-10)

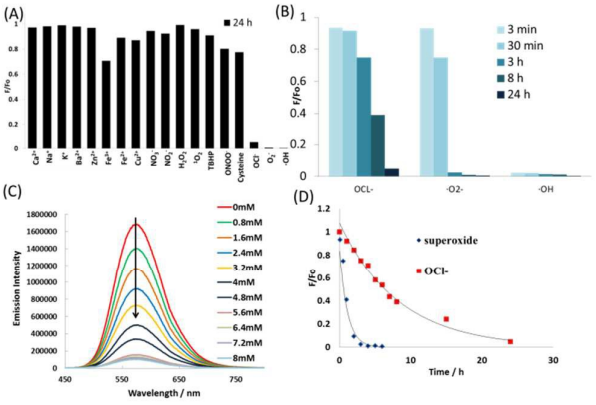

Fig. 2 (A) Fluorescence response of SPC (23 μM) to various ROSs or metal ions after t = 24 h. (B) Fluorescence response of SPC (23 μM) to OCl^-, O_2^- and $^{\cdot}OH$ under different reaction time points including t = 3 min, 30 min, 3 h, 8h or 24h. (C) Fluorescence spectral responses of SPC (23 μM) to O_2^- of varying concentrations (from 0 to 8 mM) at pH ~10. (D) Fluorescence response of SPC (23 μM) to O_2^- and OCl^- at pH ~10 as a function of time. F_0 represented the measured fluorescence intensity of 23 μM SPC probe. F_t represented the measured fluorescence intensity of 23 μM SPC probe after an addition of ROS for time t. Data were acquired at 25 °C in aqueous media, λ_{ex} = 423 nm, λ_{em} = 575 nm.

Figs. 2B and 2D show the fluorescence intensity of SPC as a function of the reaction time in the presence of OCl^-. It was found that OCl^- induced a strong fluorescence quenching of SPC, down to less than 5% of fluorescence intensity after 24 h, in addition to O_2^- and $^{\cdot}OH$. The results from HRMS analysis indicated the cleavage of double bond after the reaction, resulting in the formation of chloro-SPC with a base peak at m/z 467.2053. (Fig. S11). It is in a good agreement with the previous study.[22] The UV-vis measurements of 23 μM SPC in the presence of one of the following ROS species including H_2O_2, $^{1}O_2$, OCl^-, O_2^-, or $^{\cdot}OH$ were also performed accordingly (Fig. S12). It is clearly shown that the absorption maximum at

420 nm corresponding to the donor-acceptor π-conjugated system of SPC molecule disappeared after mixing SPC with OCl^-, $O_2^{\cdot-}$, or $^{\cdot}OH$, suggesting the disruption of the π-conjugated system. On the contrary, the same absorption peak still remains intact after mixing SPC with H_2O_2, or $^1O_2$ even after 24 h which is attributed to the poor reactivity under reaction conditions. Because of the disappearance of ^1H NMR signals of the double bond of SPC and the appearance of new mass spectroscopic peak in the HRMS studies, it is strongly convinced that the double bond of the SPC probe is cleaved by OCl^-, $O_2^{\cdot-}$, or $^{\cdot}OH$ providing the detection mechanism of this probe as shown in Scheme S2. These results clearly revealed that SPC can react with and detect three specific ROS including $^{\cdot}OH$, $O_2^{\cdot-}$ and OCl^- in solution. The formation of a stable final product by trapping a particular ROS with SPC would minimize the possibility of interference. In addition, no other side products are generated in this reaction as compared to other systems.[23-24] Thus, SPC can use to sense and detect $^{\cdot}OH$, $O_2^{\cdot-}$ and OCl^- without giving any intermediate interference signals between a strong signal and/or no signal, making it a promising candidate for direct detection of $^{\cdot}OH$, $O_2^{\cdot-}$ and OCl^- *in vivo*.

Cytotoxicity effect of SPC on macrophages

To show the potential of this probe as a ROS sensor for imaging in living cells, the cytotoxicity effect of SPC on RAW 264.7 cells was evaluated using typical MTT assay. The cell samples were incubated with different concentrations of SPC at 37 °C overnight. MTT reagent was then added to each cell sample and followed by dissolving with ethanol/DMSO (1:1). Very high cell viability was observed with more than 90% survival rate in 1.0×10^4 cells/well (Fig. S13). Interestingly, SPC was efficiently taken up by RAW 264.7 cells only. In sharp contrast, its analogous; SPM without the carboxylic acid functional group could merely be taken up by HeLa, MCF-7, KB, HepG2 and A549 cells but not the macrophages. (Fig. 3 and S14) This SPC probe also shows a remarkable photostability in macrophages under one-photon excitation as its fluorescence intensity remains fairly stable over a period of 30 min (Fig. S15). These findings highlight the uniqueness and merits of SPC as a cellular ROS probe since most of ROS generation and their chemical reactions occur in macrophages. The excellent biocompatibility of SPC in terms of low cytotoxicity and high cell permeability to macrophages is crucial to be practically useful for live cell detection/imaging.

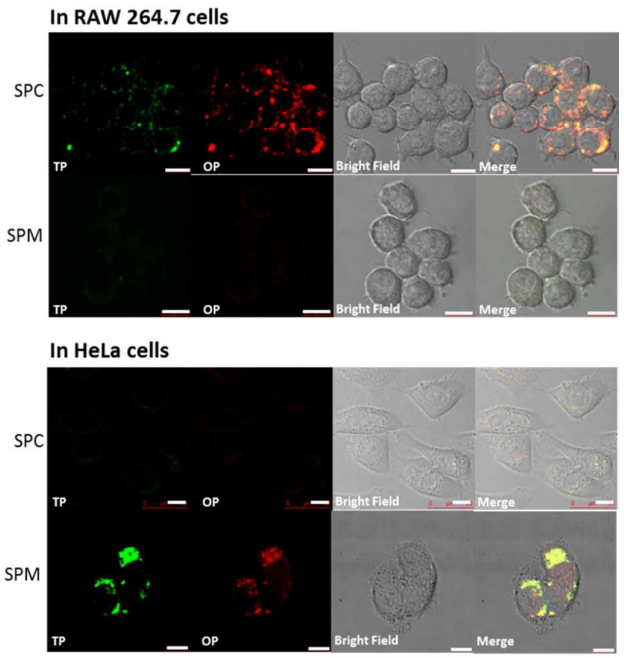

Fig. 3 Confocal fluorescence microscopy images of RAW 264.7 and HeLa cells after incubating with 23 μM of SPC or 23 μM of SPM for 24 h at 37°C. Scale bar is 10 μm.

Cellular protection effect of SPC on PMA-stimulated macrophages

To examine the practical usefulness of SPC for detecting of ROS and explore the potential of cellular protection effect, we performed the investigations in chemically-treated RAW 264.7 cells. It is well-known that phorbol-12-myristate-13-acetate (PMA) stimulated macrophages enhances the release of ROS in RAW 264.7 cells, particularly $O_2^{\cdot-}$.[25] SPC was added into 500 μL of the culture medium of RAW 264.7 macrophages (final concentration of probe was 23 μM). Then the fluorescence images of the cells were monitored after culturing with the dual-mode fluorescence probe for 6 h at 37 °C. The probe shows bright and stable one-photon (OP) and two photon (TP) fluorescence signals (Fig. 4A). After the SPC-loaded RAW 264.7 cells were stimulated with PMA (100 ng/mL) at 37 °C for 3 h, one-photon (OP) and two-photon (TP) excited fluorescence intensities were distinctly weakened as compared with the images without being stimulated with PMA (Fig. 4B). This is also in a good agreement with the results of average emission intensity obtained from cell extracts (Fig. S16). To verify selectivity of probe for intracellular $O_2^{\cdot-}$, a control experiment was performed by treating the cells with a Tiron solution (100 ng/mL), which is a known cell-permeable $O_2^{\cdot-}$ scavenger,[26] for 1 h after PMA stimulation. As anticipated, both OP and TP fluorescence channels gave bright fluorescence images, consistently implied that the fluorescence quenching response originated from the activated $O_2^{\cdot-}$ releasing in the cells (Fig. 4C). The bright-field images confirmed that the treated RAW 264.7 cells were highly viable throughout the imaging experiments. It is consistently shown that the selective response to/reaction with $O_2^{\cdot-}$ leads to the quenched

fluorescence. Importantly, this dual-mode fluorescence imaging approach provides more direct and convincing signal change as compared to other detection methods for ROS in a cellular system.[27-28]

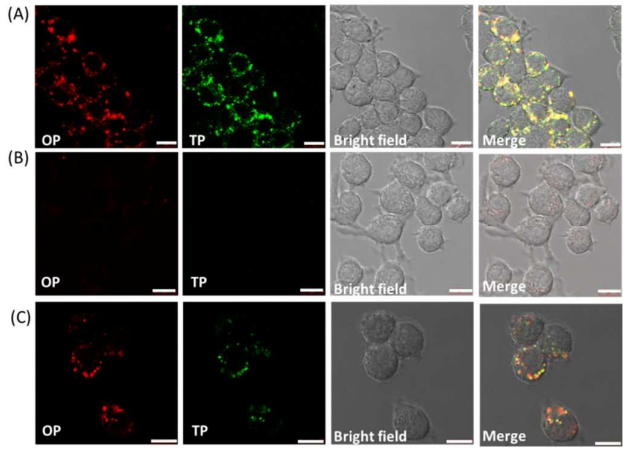

Fig. 4 Confocal one-photon (OP) and two photon (TP) fluorescence microscopy images of RAW 264.7 cells (a) with an incubation of 23 μM of SPC only, (b) with an incubation of 23 μM of SPC followed by a stimulation of PMA (100 ng/mL) at 37°C for 3 h, , (c) with a stimulation of PMA (100 ng/mL) followed by an incubation of Tiron (100ng/mL) for 1 h and SPC for another 6 h at 37°C. OP and TP images were acquired using 458 nm and 810 nm excitations, respectively. Both emissions collected from 500 – 600 nm. Scale bar is 10 μm.

In addition, it was unambiguously showed that PMA-treated RAW 264.7 cells exhibited dramatic morphology change due to their increased ROS production, but no obvious decrease in cell viability was observed (Fig. S17).[29] The spherical RAW 264.7 cells (blank) became lengthened with multiple huge pseudopodi but without vesicles after 40 min of PMA treatment. In sharp contrast, SPC molecules showed remarkably suppressing capability to prevent the morphological alternation of these PMA-stimulated cells (Fig. 5). Such suppression was attributed to the inhibition of a common pathway involved in the production of inflammatory mediators, ROS.

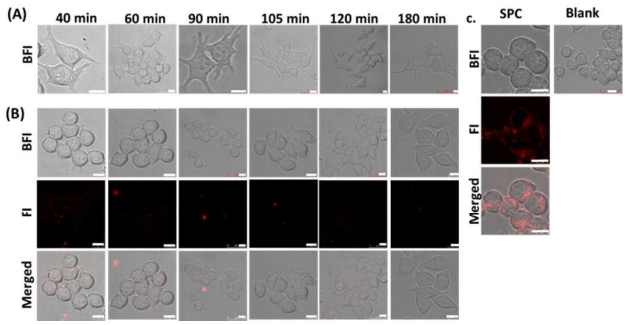

Fig. 5 Bright field images (BFI) and fluorescence images (FI) showing PMA-induced RAW 264.7 cell morphological changes as a function of time and showing SPC as ROS scavenger to prevent the morphological alternation of PMA-stimulated RAW 264.7 cells. (a) RA W 264.7 cells were treated with PMA (100 ng/mL) at 37°C for 3 h. (b) RAW 264.7 cells were incubated with 23 μM of SPC for 6 h followed by a stimulation of PMA (100 ng/mL) for 3 h at 37°C. (c) RAW 264.7 cells (Blank) and RAW 264.7 cells treated with 23 μM of SPC for 6 h. Corresponding fluorescence images showing OP fluorescence signal of SPC. Scale bar is 10 μm.

Cellular protection effect of SPC on LPS-stimulated macrophages

To further verify the applicability of SPC for cellular protection in living cells in terms of reacting with excess ROS, the RAW 264.7 cells were also treated with lipopolysaccharide (LPS), commonly used for eliciting immune responses in mammalian cells and producing highly reactive OCl^-.[30-31] In this experiment, the SPC-loaded RAW 264.7 cells were incubated with LPS (5 mg/mL) for 14 h to produce endogenous OCl^-. Under these conditions, the OP and TP fluorescence signals of SPC diminished dramatically, suggesting that SPC had successfully detected and quenched by OCl^- generated under LPS stimulation (Fig. 6A). In addition, the LPS-stimulated RAW 264.7 cells simultaneously induced high cytotoxicity (Fig. S18, blue curve) and morphological change to polygonal shape with numerous pseudopodi and vesicles (Fig. 6B) upon increasing the LPS concentrations. Live/dead assay including propidium iodide (PI) staining and/or trypan blue staining was used to evaluate the cell viability as a function of LPS concentration. As anticipated, LPS-stimulated RAW 264.7 cells exhibited a significant cell death when LPS concentration was above 10 ng/mL. However, in the presence of SPC, LPS-stimulated RAW 264.7 cells dramatically reduced cell death even LPS concentration was above 100 ng/mL. (Fig. S18, red curve and Fig. 6C). These results revealed the final product formed after reacting of SPC with OCl^- is non-toxic and preserve the cell viability. Thus, SPC showed protection effect to mitigate the LPS-induced cytotoxicity and enhance viability of RAW 264.7 cells in a dose-dependent manner. To the best of our knowledge, this is the first example of using a bifunctional two-photon fluorescent probe to detect and image two distinct ROS species, O_2^- and OCl^- in macrophages. Together with a low cytotoxicity and a high cellular protection capability, this work has demonstrated the effectiveness and versatility of this carbazole-based cyanine as a smart ROS sensor for intracellular detection of O_2^- and OCl^- in a biological system and also as a ROS scavenger for cellular protection in stimulated macrophages.

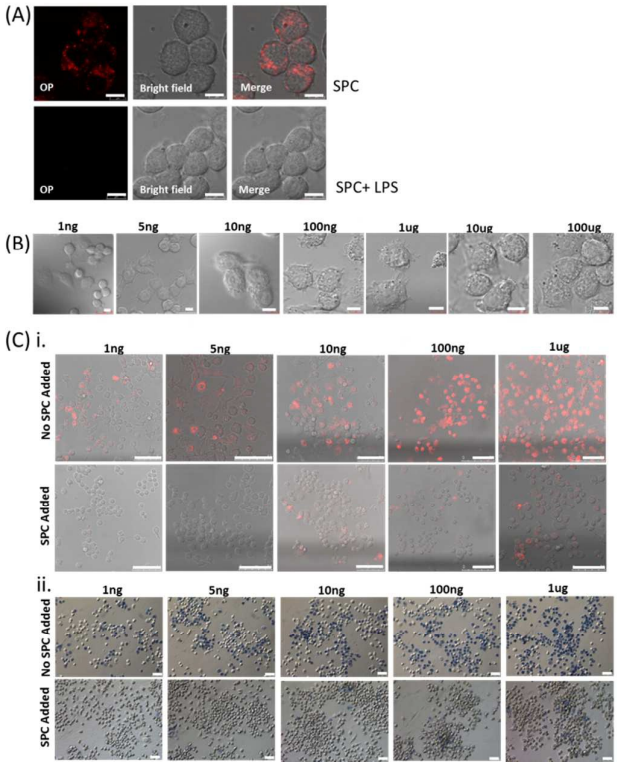

Fig. 6 (a) Confocal one-photon (OP) fluorescence microscopy images of RAW 264.7 cells with an incubation of 23 μM of SPC followed by a stimulation of LPS (100 ng/mL) at 37°C for 12 h. Scale bar is 10 μm. (b) Bright field images showing LPS-induced cell morphological changes under different concentrations of LPS. Cytoplasm vacuoles were observed in RAW 264.7 cells treated with more than 100 ng/mL LPS. Scale bar is 10 μm. (c) (i) Bright-field images showing PI staining of LPS-treated RAW 264.7 cells and (ii) bright-field images showing trypan blue staining of LPS-treated RAW 264.7 cells before and after adding 23 μM of SPC as a function of concentration of LPS. Scale bar is 50 μm.

Conclusions

In summary, a novel biocompatible and macrophage cell-membrane permeable carbazole-based cyanine has been developed which has shown to be an effective and versatile one-photon and two-photon fluorescent probe for detection of three biologically important ROS, namely $^{\cdot}OH$, O_2^- and OCl^- in aqueous buffer solution. In addition, this probe has found to be useful in reacting with intracellular O_2^- and OCl^- in macrophage and preventing RAW 264.7 cells from the PMA-induced morphological changes as well as in mitigating the LPS-induced cytotoxicity of RAW 264.7 cells. Importantly, this is the first example of a two-photon cellular ROS sensor and scavenger for ROS detection and cellular protection in stimulated macrophages. Further development of multifunctional cyanine probe for intracellular detection and protection of ROS in a specific organelle is currently under investigation.

Experimental section

Materials

Lipopolysaccharide (LPS), phorbol-12 myristate-13 acetate (PMA), Tiron, diethylenetriamine pentaacetic acid, potassium superoxide and 12 M hydrochloric acid were used as purchased from Sigma-Aldrich. Sodium molybdate, sodium nitrite, sodium hydroxide, calcium chloride, sodium chloride, zine chloride, potassium chloride and barium chloride were purchased from J&K. 37% of hydrogen peroxide was purchased from UNI-CHEM. Sodium hypochlorite was purchased from Acros Organics. Fetal bovine serum (FBS), phosphate buffered saline (PBS), Dulbecco's Modified Eagle Medium (DMEM) and penicillin streptomycin solution were purchased from Invitrogen.

Instrumentation

Absorbance, emission, stability and quenching of SPC in different solutions were characterized by UV-VD (Agilent 8453) and Spectrofluorometer (Fluormax-4). Confocal fluorescence imaging and bright field imaging were performed on Laser Confocal Scanning Microscope (Leica TCS SP5) with magnification of 63X. The MTT experiment was conducted at Bio Tek Powerwave XS microplate reader. ^{1}H NMR and ^{13}C NMR spectra were recorded using a Bruker-400 NMR spectrometer. Mass spectroscopy (MS) measurements were carried out by fast atom bombardment on the API ASTER Pulser I Hybrid Mass Spectrometer or matrix-assisted laser desorption ionization-time-of-flight (MALDI-TOF) technique.

Synthetic procedures of SPC

(E)-1-(carboxymethyl)-4-(2-(9-(2-(2-methoxyethoxy)ethyl)-9H-carbazol-3-yl)vinyl)pyridin-1-ium bromide (SPC) A solution of 4 (0.17 g, 0.5 mmol) and bromoacetic acid (0.28 g, 2.0 mmol) in ethanol was stirred overnight at room temperature. After removing the solvent, the residue was precipitated from methanol and ethyl acetate to afford SPC in 83% yield. ^{1}H NMR (400 MHz, DMSO-d_6) δ 8.68 (d, *J* = 5.2 Hz, 2H), 8.56 (s, 1H), 8.11-8.19 (m, 4H), 7.86 (dd, *J* = 1.2 Hz, *J* = 8.4 Hz, 1H), 7.72 (d, *J* = 8.8 Hz, 1H), 7.67 (d, *J* = 8.4 Hz, 1H), 7.51-7.53 (m, 1H), 7.47-7.49 (m, 1H), 7.27 (t, *J* = 7.2, 1H), 4.84 (s, 2H), 4.58 (t, *J* = 5.2 Hz, 2H), 3.81(t, *J* = 5.2 Hz, 2H), 3.44-3.47 (m, 2H), 3.30-3.28 (m, 2H), 3.10 (s, 3H). ^{13}C NMR (100 MHz, $CDCl_3$) δ170.4, 152.7, 144.8, 141.9, 141.7, 140.9, 126.4, 126.3, 126.1, 122.7, 122.2, 122.1, 120.9, 120.3, 120.1, 119.7, 110.4, 110.2, 71.3, 69.8, 68.8, 58.1, 42.9; HRMS (MALDI-TOF) m/z Calcd for $C_{26}H_{27}N_2O_4$ 431.1965 Found 431.1953[M^+].

Preparation of ROS and metal ion solutions

Various ROSs and metal ion solutions have been prepared according to the previously reported methods. [i] Detail preparation information is the following:

Various metal ion solutions: 8 mM of different types of cations including Ca^{2+}, Na^+, K^+, Ba^{2+}, Fe^{3+}, Fe^{2+} and Cu^{2+} were prepared from commercially available metals chloride. **Singlet oxygen**: Singlet oxygen was generated by mixing sodium molybdate dehydrate with H_2O_2 at molar ratio of 1 : 2 under pH range from 9.5 to 11.5. **Hydrogen peroxide:** 8 mM hydrogen peroxide was generated by diluting 37% H_2O_2. The final concentration of H_2O_2 was determined by its absorbance at 240 nm (ε = 43.6 $M^{-1}cm^{-1}$) **Hypochlorite anions**: 8 mM OCl^-

was prepared by diluting concentrated commercially available NaOCl. The concentration of OCl^- was determined by its absorbance at 292 nm (ε = 350 $M^{-1}cm^{-1}$). **Superoxide**: 8 mM superoxide was initially prepared by dissolving KO_2 in 50 mM ice-cold NaOH solution and then mixing with 0.5 mM diethylenetriamine pentaacetic acid. **Peroxynitrite**: 8 mM nitrite and nitrate anions were prepared from sodium nitrite and sodium nitrate. ***Tert*-butyl hydroperoxide** 100 μM of *Tert*-butyl hydroperoxide was mixed with 0.1 M sodium phosphate buffer at 37°C, pH 7.4 followed by adding 0.1% DMF as co-solvent. **Cysteine**: 8 mM cysteine solution was prepared from commercially available cysteine. **Hydroxide radical:** 8 mM of Iron(II) perchlorate and 37% hydrogen peroxide were mixed and added up to total volume of 5 mL with D. I. water. The ratio of H_2O_2 to Fe^{2+} is 10:1 through the Fenton reaction.

Acknowledgements

This work was financially supported by the CityU Start-up Grant 7200300, CityU Strategic Research Grant 9616302 and 7004026, and National Science Foundation of China 21324077. This work was also supported by GRF (HKBU 203212), Hong Kong Research Grant Council and Institute of Molecular Functional Materials which was supported by a grant from the University Grants Committee, Areas of Excellence Scheme (AoE/P-03/08).

Notes and references

1 B. C. Dickinson, D. Srikun and C. J. Chang, *Curr. Opin. Chem. Biol.,* 2010**, 14,** 50.
2 A. Matsuzawa, K. Saegusa, T. Noguchi, C. Sadamitsu, H. Nishitoh, S. Nagai, S. Koyasu, K. Matsumoto, K. Takeda and H. Ichijo, *Nat. Immuno.,* 2005, **6**, 587.
3 Q. Li, M. M. Harraz, W. Zhou, L. N. Zhang, W. Ding, Y. Zhang, T. Eggleston, C. Yeaman, B. Banfi and J. F. Engelhardt, *Mol. Cell Biol.,* 2006, **26**, 140–154.
4 H. K. Seitz and F. Stickel, *Nat. Rev. Cancer.,* 2007, **7**, 599.
5 G. K. Hansson and P. Libby, *Nat. Rev. Immunol.,* 2006, **6**, 508.
6 L. Galluzzi, K. Blomgren and G. Kroemer*, Nat. Rev. Neurosci.,* 2009, **10**, 481.
7 J. M. N. McCord, *Engl. J. Med.,* 1985**, 312,** 159.
8 E. G. Janzen, L. T. Jandristis, R. V. Shetty, D. L. Haire and J. W. Hilborn, *Chem. Biol. Interact.,* 1989**, 70,** 167.
9 E. G. Janzen, Methods Enzymol., 1984**, 105,** 188.
10 G. Chen, F. Song, J. Wang, Z. Yang, S. Sun, J. Fan, X. Qiang, X. Wang, B. Dou and X. Peng, *Chem. Commun.,* 2012, **48**, 2949.
11 H. M. Kim, M. J. An, J. H. Hong, B. H. Jeong, O. Kwon, J.Y. Hyon, S. C. Hong, K. J. Lee and B. R. Cho, *Chem. Commun.,* 2009, **47**, 7422.
12 F. Helmchen and W. Denk, *Nat. Meth.,* 2005, **2**, 932.
13 D. Kim, H. G.Ryu, K.H. Ahn, *Org. Biomol. Chem.*, 2014,**12**, 4550-4566.
14 J. H. Lee, C. S. Lim, Y. S. Tian, J. H. Han and B. R. Cho, *J. Am. Chem. Soc.,* 2010, **132**, 1216.
15 W. Zhang, Li, P. F. Yang, X. Hu, C. Sun, W. Zhang, D. Chen and B. Tang, *J. Am. Chem. Soc.,* 2013, **135**, 14956.
16 P. Li, W. Zhang, K. Li, X. Liu, H. Xiao, W. Zhang and B. Tang, *Anal. Chem.,* 2013, **85**, 9877.
17 H. Guo, H. Aleyasin, S. S. Howard, B. C. Dickinson, V. S. Lin, R. E. Haskew-Layton, C. Xu, Y. Chen and R. R. Ratan*, J. Biomed. Opt.,* 2013, **18**, 1060021.
18 M. K. Kim, C. S. Lim, J. T. Hong, J. H. Han, H. Y. Jang, H. M. Kim and B. R. Cho, *Angew. Chem. Int. Ed.,* 2010, **49**, 364.
19 X. J. Feng, P. L. Wu, F. Bolze, H. W. C. Leung, K. F. Li, N. K. Mak, D. W. J. Kwong, J. F. Nicoud, K. W. Cheah and M. S. Wong, *Org. Lett.,* 2010**, 12**, 2194.
20 W. Yang, Y. Wong, O. T. W. Ng, L. P. Bai, D. W. J. Kwong, Y. Ke, Z. H. Jiang, H. W. Li, K. K. L. Yung and M. S. Wong, Angew. Chem. Int. Ed., 2012, 51, 1804.
21 W. Yang, P. S. Chan, M. S. Chan, K. F. Li, P. K. Lo, N. K. Mak, K. W. Cheah and M. S. Wong, *Chem. Commun.,* 2013, **49**, 3428.
22 S. Chen, J. Lu, C. Sun, H. Ma, *Analyst*, 2010, **135**, 577.
23 X. Chen, X. Wang, S. Wang, W. Shi, K. Wang and H. Ma, *Chem. Eur. J.,* 2008, **14**, 4719.
24 D. P. Murale, H. Kim, W. S. Choi and D. G. Churchill, Org. Lett., 2013, 15, 3630.
25 D. Oushiki, H. Kojima, T. Terai, M. Arita, K. Hanaoka, Y. Urano and T. Nagano, *J. Am. Chem. Soc.,* 2010, **132**, 2795–2801.
26 K. Xu, X. Liu, B. Tang, G. Yang, Y. Yang and L. An, *Chem. Eur. J.,* 2007**, 13,** 1411.
27 T. H. Tsai, K. C. Lin and S. M. Chen, *Int. J. Electrochem. Sci.,* 2011, **6**, 2672.
28 F. J. Huo, J. J. Zhang, Y. T. Yang, J. B. Chao, C. X. Yin, Y. B. Zhang and T. G. Chen, *Sensors & Actuators: B. Chemical,* 2012, **166**, 44.
29 S. Y. Lee and J. Y. Cho, *BMB Rep.,* 2009, **42**, 574.
30 L. Yuan, W. Lin, Y. Xie, B. Chen and J. Song, *Chem. Eur. J.,* 2012, **18**, 2700.
31 G. Li, D. Zhu, Q. Liu, L. Xue and H. Jing, *Org. Lett.,* 2013**, 15,** 2002.